

Article

Tissue-Specific Vulnerability to Apoptosis in Machado-Joseph Disease

Ana F. Ferreira ^{1,2}, Mafalda Raposo ², Emily D. Shaw ³, Naila S. Ashraf ³, Filipa Medeiros ¹, Maria de Fátima Brilhante ^{1,4}, Matthew Perkins ³, João Vasconcelos ⁵, Teresa Kay ⁶, Maria do Carmo Costa ^{3,*,†} and Manuela Lima ^{1,2,*,†}

- ¹ Faculdade de Ciências e Tecnologia, Universidade dos Açores, 9500-321 Ponta Delgada, Portugal
² Instituto de Biologia Molecular e Celular (IBMC), Instituto de Investigação e Inovação em Saúde (i3S), Universidade do Porto, 4200-135 Porto, Portugal
³ Department of Neurology, Michigan Medicine, University of Michigan, Ann Arbor, MI 48109, USA
⁴ Centro de Estatística e Aplicações, Universidade de Lisboa (CEAUL), 1749-016 Lisboa, Portugal
⁵ Serviço de Neurologia, Hospital do Divino Espírito Santo (HDES), 9500-370 Ponta Delgada, Portugal
⁶ Serviço de Genética Clínica, Hospital D. Estefânia, 1169-045 Lisboa, Portugal
* Correspondence: mariadoc@med.umich.edu (M.d.C.C.); maria.mm.lima@uac.pt (M.L.); Tel.: +1-734-764-4094 (M.d.C.C.); +351-296650118 (M.L.)
† These authors contributed equally to this work.

Abstract: Machado-Joseph disease (MJD) is a dominant neurodegenerative disease caused by an expanded CAG repeat in the *ATXN3* gene encoding the ataxin-3 protein. Several cellular processes, including transcription and apoptosis, are disrupted in MJD. To gain further insights into the extent of dysregulation of mitochondrial apoptosis in MJD and to evaluate if expression alterations of specific apoptosis genes/proteins can be used as transcriptional biomarkers of disease, the expression levels of *BCL2*, *BAX* and *TP53* and the *BCL2/BAX* ratio (an indicator of susceptibility to apoptosis) were assessed in blood and post-mortem brain samples from MJD subjects and MJD transgenic mice and controls. While patients show reduced levels of blood *BCL2* transcripts, this measurement displays low accuracy to discriminate patients from matched controls. However, increased levels of blood *BAX* transcripts and decreased *BCL2/BAX* ratio are associated with earlier onset of disease, indicating a possible association with MJD pathogenesis. Post-mortem MJD brains show increased *BCL2/BAX* transcript ratio in the dentate cerebellar nucleus (DCN) and increased *BCL2/BAX* insoluble protein ratio in the DCN and pons, suggesting that in these regions, severely affected by degeneration in MJD, cells show signs of apoptosis resistance. Interestingly, a follow-up study of 18 patients further shows that blood *BCL2* and *TP53* transcript levels increase over time in MJD patients. Furthermore, while the similar levels of blood *BCL2*, *BAX*, and *TP53* transcripts observed in preclinical subjects and controls is mimicked by pre-symptomatic MJD mice, the expression profile of these genes in patient brains is partially replicated by symptomatic MJD mice. Globally, our findings indicate that there is tissue-specific vulnerability to apoptosis in MJD subjects and that this tissue-dependent behavior is partially replicated in a MJD mouse model.

Keywords: polyglutamine disease; spinocerebellar ataxia type 3; SCA3; MJD; *ATXN3*; ataxin-3; biomarkers; mitochondrial apoptosis; human brains; transgenic mice



Citation: Ferreira, A.F.; Raposo, M.; Shaw, E.D.; Ashraf, N.S.; Medeiros, F.; Brilhante, M.d.F.; Perkins, M.; Vasconcelos, J.; Kay, T.; Costa, M.d.C.; et al. Tissue-Specific Vulnerability to Apoptosis in Machado-Joseph Disease. *Cells* **2023**, *12*, 1404. <https://doi.org/10.3390/cells12101404>

Academic Editor: Takahiro Seki

Received: 7 April 2023

Revised: 10 May 2023

Accepted: 11 May 2023

Published: 17 May 2023



Copyright: © 2023 by the authors. Licensee MDPI, Basel, Switzerland. This article is an open access article distributed under the terms and conditions of the Creative Commons Attribution (CC BY) license (<https://creativecommons.org/licenses/by/4.0/>).

1. Introduction

Machado-Joseph disease/spinocerebellar ataxia type 3 (MJD/SCA3) (OMIM#109150) is the most frequent autosomal dominant inherited ataxia worldwide [1]. MJD is caused by an expansion of a polyglutamine (polyQ)-encoding CAG repeat in the *ATXN3* gene [2]. Ataxin-3 (*ATXN3*), the protein encoded by *ATXN3*, is ubiquitously expressed in different cell types of peripheral and central nervous system tissues [3]. Neuropathological complexity is a characteristic of this disease, which especially affects the cerebellum, brainstem,

basal ganglia, some cranial nerves, and spinal cord [4]. In average, the age at onset of MJD has been reported around 40 years old, and the mean survival time is estimated to be 21 years [5]. In MJD, overt disease is preceded by a preclinical phase in which neuropathological and molecular alterations are already present [6–9].

Several studies using cellular and animal models of MJD, including the YACMJDQ84.2 (Q84) transgenic mice that are frequently used in pre-clinical studies of MJD [10–14], have been revealing that mutant ATXN3 harboring an expanded polyQ tract is involved in the impairment of transcription, mitochondrial function, mechanisms regulating oxidative stress, and apoptosis [3,15,16]. Several of these changes, including transcriptional dysregulation, have also been observed in blood samples from MJD carriers [17,18].

Mitochondrial apoptosis is a complex mechanism regulated by several proteins including those belonging to the BCL2 family, such as the anti-apoptotic protein BCL2 (B-cell lymphoma-2) and the pro-apoptotic protein BAX (BCL2 Associated X) [19]. Another crucial player in apoptosis is the transcription factor P53 (Tumor protein p53) which, among other roles, regulates the levels and the activity of BCL2 family proteins [20]. In fact, evidence of a direct link between mutant ATXN3 and apoptosis has been provided by Liu and colleagues [21] who reported that p53 is a substrate of ATXN3 and that mutant ATXN3, exhibiting a stronger deubiquitinase activity than native ATXN3, increases p53 stability and its consequent cellular accumulation leading to increased p53-dependent apoptosis in a MJD zebrafish model and in HCT116 cells. Moreover, our group has formerly shown that peripheral blood cells of MJD carriers display decreased *BCL2/BAX* transcript ratio [8] resulting from a reduction of blood *BCL2* transcript levels [18], indicating a higher vulnerability to an apoptotic stimulus in MJD subjects compared with controls. Similarly, at the protein level, abundance of Bcl2 and Bcl2/Bax ratio has been found to be decreased in human neuronal SK-N-SH cells expressing expanded-polyQ ATXN3 compared with the parental cells [22]. Although some studies using animal and cellular models have shown the involvement of neuronal apoptosis in MJD [22,23], little is known about the expression patterns of apoptotic-related genes in the brain and other tissues of individuals with MJD [24].

Hence, the levels of the apoptosis related *BCL2*, *BAX* and *TP53* transcripts in cross-sectional and longitudinal samples of peripheral blood from MJD carriers (patients and pre-clinical subjects) were assessed to gather further insights into the dysregulation of mitochondrial apoptosis in MJD and to evaluate their capacity of being used as transcriptional biomarkers of MJD. Additionally, the expression patterns of *BCL2*, *BAX* and *TP53* genes were investigated in samples from post-mortem brains of MJD patients to better elucidate the involvement of the mitochondrial apoptosis pathway in MJD pathogenesis and to evaluate possible conserved changes of apoptosis markers in the brain and peripheral blood of MJD patients. Finally, the transcript and protein levels of mouse *Bcl2*, *Bax* and *Trp53* genes were evaluated in samples from the peripheral blood and the brain of Q84 transgenic mice, expressing the full-length human disease *ATXN3* gene, to determine whether this widely used MJD mouse model replicates the findings observed in MJD subjects.

2. Materials and Methods

2.1. Human Samples and Clinical Data

A total of 19 preclinical (no ataxia or diplopia) subjects, 42 MJD patients and 63 healthy controls were included in this study. A summarized clinical, genetic, and demographic characterization of the individuals included in this study is provided in Supplementary Table S1.

Blood samples: baseline samples from 19 preclinical subjects, 37 patients and 54 age (± 3 years) and sex-matched paired controls were used in a cross-sectional study to evaluate the expression levels of *BCL2*, *BAX* and *TP53* transcripts (Figure 1(A1); Supplementary Table S1). A subset of 13 patients with five or less years of disease duration was used to represent the early stage of the disease (early patients) (Figure 1(A1)). The cut-off used to define the early patients was based on the natural history data for MJD that shows

that the mean score of disease progression (defined by gait impairment) evolves very slowly during the first five years [25]. Additionally, for a subset of 18 MJD patients, blood samples collected at one or two additional observational moments were used in a follow-up study (Figure 1(A1); Supplementary Table S2). All MJD subjects underwent a standard neurological evaluation by the same single neurologist. Age at onset was defined as the age of appearance of the first symptoms (gait ataxia and/or diplopia) reported by the patient or a close relative. Disease duration was defined as the time elapsed between age at onset and age at neurological evaluation/blood collection. Preclinical subjects were enrolled in the study after being confirmed as carriers of the *ATXN3* mutation, in the context of the Azorean Genetic Counseling and Predictive Test Program offered by the regional health system to patients and families. For preclinical subjects, the number of years between the age at neurological evaluation/blood collection and the predicted age at disease onset (years to onset, time) was calculated as previously described by Raposo and colleagues [26]. The determination of the number of CAG repeats at the *ATXN3* locus was performed for all MJD subjects as described by Bettencourt and colleagues [27]. In addition to the lack of family history of MJD, most of the controls were molecularly excluded for the *ATXN3* mutation using the above-mentioned protocol [27]. The use of blood samples and clinical data of MJD carriers for the purposes of this study was approved by the Ethics Committee of the University of the Azores (Parecer 5/2017 and Parecer 26/2018). All subjects provided written informed consent for research.

Brain samples: frozen samples from post-mortem brain regions of deidentified and molecularly confirmed MJD patients ($n = 5$) and molecularly excluded control subjects ($n = 9$) were obtained from the University of Michigan Brain Bank (Supplementary Table S1; Supplementary Table S3) and were used in a cross-sectional study (Figure 1(A2)). Samples from two brain regions severely affected in MJD (dentate cerebellar nucleus (DCN) and pons) [4] and from a region with a lower degree of disease affectation (frontal cortex) [28,29], were used in this study. The *ATXN3* CAG repeat number of all post-mortem brain samples was determined at Laragen Inc. (Culver City, CA, USA) by DNA fragment analysis (Supplementary Table S3). The use of post-mortem brain samples for the purposes of this study was approved by the University of Michigan Biosafety Committee (IBCA00000265) and by the Ethics Committees of the University of the Azores (Parecer 26/2018).

2.2. Mouse Samples

Hemizygous YACMJD84.2 (Q84) and wild-type (wt) littermate mice [30] were generated and maintained at the University of Michigan in a C57BL/6J background strain [10,14]. Mice were housed in cages with a maximum of five animals (range 3–5) and maintained in a standard 12 h light/dark cycle with food and water ad libitum. Hemizygous Q84 mice show a reduced locomotor and exploratory activity on an open-field test at least at 75 weeks of age (≈ 17 months-old-MO) [10]. At least at eight weeks of age, hemizygous Q84 transgenic mice show some neuropathological features of MJD compared to non-transgenic littermates, such as progressive intranuclear accumulation of *ATXN3* in neurons of several brain regions that are known to be also affected in MJD patients [10]. Pre-symptomatic 9 months-old (MO) Q84 ($n = 11$) and wt mice ($n = 11$), and symptomatic 18 MO Q84 ($n = 4$) and wt mice ($n = 5$) were used in the present study (Figure 1B; Supplementary Table S4). Mouse genotyping for the presence of the human disease *ATXN3* transgene was performed using DNA isolated from tail biopsy at the time of weaning, as previously described by Costa and colleagues [10] and confirmed using DNA extracted from the tail collected post-mortem. The mouse *ATXN3* CAG repeat size was determined as above mentioned for human brain samples. Animal procedures were approved by the University of Michigan Committee on Use and Care of Animals (Protocol PRO00006371). The use of animal samples for the purposes of this study was approved by the Ethics Committees of the University of the Azores (Parecer 26/2018).

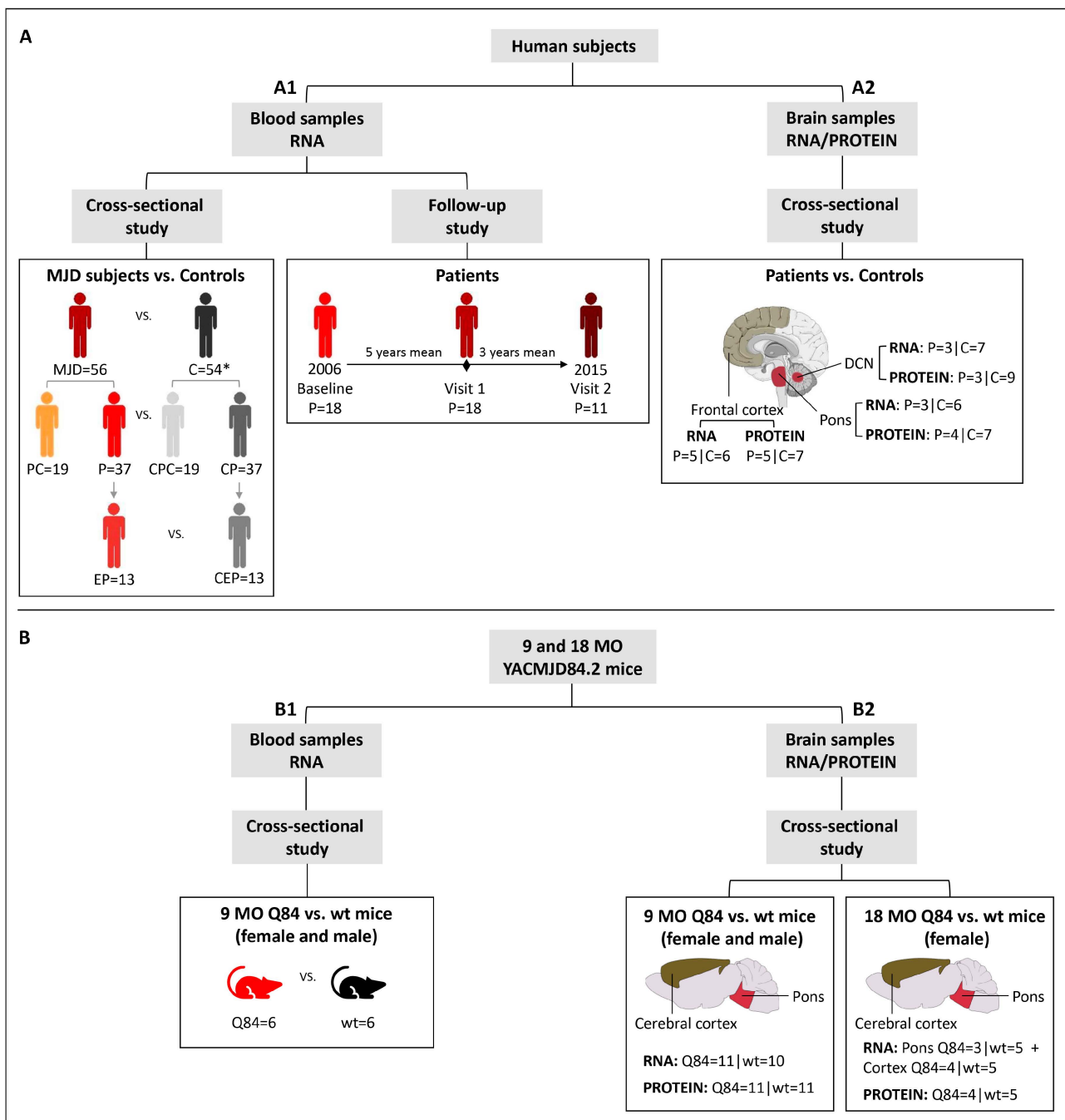


Figure 1. Design of the study: *BCL2*, *BAX* and *TP53* transcript and protein levels were assessed in (A) human subjects and in the (B) YACMJD84.2 (Q84) mouse model. In human subjects, the expression levels were analyzed in (A1) blood samples from MJD carriers (preclinical subjects and patients) and controls in a cross-sectional study and from patients in a follow-up study, and in (A2) brain samples from MJD patients and controls in a cross-sectional study (brain figure was partly generated using Servier Medical Art, provided by Servier, licensed under a Creative Commons Attribution 3.0 unported license). Expression levels of the mouse homologue *Bcl2*, *Bax*, and *Trp53* genes were analyzed in (B1) blood samples from 9-month-old (MO) Q84 transgenic and wild-type (wt) littermate mice and in (B2) brain samples from 9 and 18 MO Q84 transgenic and wt mice. MJD, MJD subjects; PC, preclinical subjects; P, patients; EP, early patients; C, controls; CPC, controls of PC subjects; CP, controls of patients; CEP, controls of early patients. * two control individuals were included in both CPC and CP groups.

Blood samples: mice were anesthetized with ketamine/xylazine, blood was collected from a subset of the 9 MO mice (Q84 = 6 and wt = 6) (Figure 1(B1)) with a sterile syringe by cardiac puncture, and RNAlater Stabilization Solution (Thermo Fisher Scientific, Waltham, MA, USA) was added to the blood and stored at -20°C . Mice were subsequently perfused transcardially with phosphate-buffered saline.

Brain samples: 9 MO (Q84 = 11 and wt = 11) and 18 MO (Q84 = 4 and wt = 5) mouse brains (Figure 1(B2)) were collected after saline perfusion, dissected in the two hemispheres, and the pons and cerebral cortex (isocortex) regions were macro dissected and stored at -80°C . Brain tissues from the right hemisphere were used for RNA studies and tissues from the left hemisphere were used for protein studies.

2.3. RNA Extraction and cDNA Synthesis

Human samples: total RNA was extracted from blood samples according to the procedures described in Raposo and colleagues [17]. cDNA was generated from $0.5\ \mu\text{g}$ of total RNA using the High-Capacity cDNA Reverse Transcription Kit (Applied Biosystems, Waltham, MA, USA). For post-mortem brain samples, total RNA was extracted using Trizol (Invitrogen, Waltham, MA, USA), and purified using the RNeasy mini kit (Qiagen, Hilden, Germany) as previously described [10]. RNA concentration and integrity were assessed using the Agilent 2100 Bioanalyzer (Supplementary Table S3). cDNA was generated from $1.25\ \mu\text{g}$ of total RNA using the iScript cDNA synthesis kit (BIORAD, Hercules, CA, USA).

Mouse samples: total RNA from mouse blood samples was extracted using the RiboPure RNA Purification Kit (Invitrogen). Total RNA from brain regions was extracted, quantified, and evaluated for integrity as described above for post-mortem human brain samples.

2.4. Quantitative Real-Time PCR

Human samples: qPCR experiments were conducted using the SensiFAST Probe Hi-ROX Master Mix (Bioline, Saint Petersburg, Russia) and the TaqMan Gene Expression Assays (Applied Biosystems) for *BCL2* (Hs00608023_m1), *BAX* (Hs00180269_m1) and *TP53* (Hs01034249_m1) using an ABI StepOnePlus Real-Time PCR System (Applied Biosystems). Each sample was run in triplicate (blood) or quadruplicate (brain) alongside with the respective reference gene in the same plate. Experiments including the subset of patients used in the follow-up study were performed by including the samples from a given subject corresponding to all available collection moments in the same plate. In qPCR experiments using RNA from blood samples and post-mortem brain samples, *TRAP1* (TNF receptor associated protein 1; Hs00972326_m1) [31] and *GAPDH* (glyceraldehyde 3-phosphate dehydrogenase; Hs02758991_g1) were, respectively, used as reference genes. The relative expression values were calculated using the $2^{-\Delta\text{Ct}}$ method [32] in DataAssist v3.0 software (Applied Biosystems).

Mouse samples: the qPCR experiments using mouse blood and brain samples were conducted as above described for human blood samples, using the following TaqMan Gene Expression Assays (Applied Biosystems) for *Bcl2* (B cell leukemia/lymphoma 2; Mm00477631_m1), *Bax* (BCL2-associated X protein; Mm00432051_m1) and *Trp53* (transformation related protein 53; Mm01731287_m1). For both blood and brain samples, *Hmbs* (hydroxymethylbilane synthase; Mm01143545_m1) was used as the reference gene.

2.5. Western Blotting

Human samples: protein extracts from DCN, the pons and frontal cortex tissues were obtained by homogenization in cold phosphate-buffered saline (PBS) containing protease inhibitor cocktail (cOmplete Protease Inhibitor Cocktail, Roche) and phosphatase inhibitors (PhosSTOP, Roche, Basel, Switzerland), followed by sonication and centrifugation. The supernatant was collected (PBS-soluble fraction) and stored at -80°C . The pellet was resuspended in 1% sodium lauroyl sarcosinate (sarkosyl, Sark)/PBS, sonicated, centrifuged and the supernatant (sarkosyl-soluble fraction) was stored at -80°C . Total protein concentrations from PBS-soluble (soluble) and sarkosyl-soluble (insoluble) fractions were assessed

using the BCA method (Pierce BCA Protein Assay Kit; Thermo Fisher Scientific). Total protein lysates from PBS-soluble fractions and sarkosyl-soluble fractions (50 µg) were resolved on 12% SDS-PAGE gels, and corresponding polyvinylidene difluoride (PVDF) membranes were incubated overnight at 4 °C with various antibodies: rabbit anti-Bcl-2 (1:500; #3498, Cell Signaling, Danvers, MA, USA), rabbit anti-Bax (1:500; #2772, Cell Signaling) mouse anti-p53 (1:1000; #2524, Cell Signaling), mouse anti-GAPDH (1:10,000; MAB374, Millipore, Burlington, MA, USA), and mouse anti-ATXN3 (1H9) (1:2000; MAB5360, Millipore). Bound primary antibodies were visualized by incubation with peroxidase affiniPure goat anti-rabbit or anti-mouse secondary antibody (1:10,000; Jackson Immuno Research Laboratories, West Grove, PA, USA), followed by reaction with ECL-plus reagent (Western Lighting, PerkinElmer, Waltham, MA, USA) and subsequent exposure to autoradiography films. Film band intensity was quantified by densitometry on ImageJ.

Mouse samples: protein extraction and quantification from the pons and cerebral cortex from 9 and 18 MO Q84 and wt mice was conducted as previously described for post-mortem human brain samples. Total protein lysates from PBS-soluble and sarkosyl-soluble fractions (40–75 µg) of each brain region were resolved on 12% SDS-PAGE gels.

2.6. Statistical Analysis

2.6.1. Cross-Sectional Studies

Human samples: blood transcript levels of MJD subjects were compared to those of controls using a T-test. When considering the groups of preclinical subjects and patients individually, blood transcript levels were compared to age- and sex-matched paired controls using a Wilcoxon Signed-rank test (two-tailed). The sex of preclinical subjects and patients was compared using a Chi-square test, and age at blood collection and the expanded CAG repeat size were compared using a Mann–Whitney U test (two-tailed). The ability for blood transcript levels to discriminate MJD subjects from healthy controls was assessed using the receiver operating characteristics (ROC) curve analysis; ROC curve accuracy was measured by the area under the curve (AUC) (95% confidence interval (CI), *p*-value). Correlations between blood transcript levels and clinical features of MJD carriers were conducted using the Spearman's rank correlation (two-tailed); a partial correlation (two-tailed) was used to adjust for covariates, whenever necessary. Post-mortem brain transcripts and protein levels were compared between biological groups (patients and controls) using a generalized linear model adjusting to the age at death.

Mouse samples: blood and brain transcript and protein levels of Q84 and wt mice (9 MO males and females combined) were compared using a Mann–Whitney U test (two-tailed).

GraphPad Prism version 8.0.1 for Windows (GraphPad Software, San Diego, CA, USA) was used to identify extreme outliers (ROUT method $Q = 1\%$), which were excluded from data analysis, and to generate the data cross-sectional graphs. Statistical analysis was performed using IBM SPSS Statistics for Windows, version 25 (IBM Corp., Armonk, NY, USA). Statistical significance was set at $p < 0.05$.

2.6.2. Follow-Up Study of Human Blood Samples

A total of 18 MJD patients were included in the follow-up study. Since repeated observations were performed on the same subjects over a period of 9 years (2006 to 2015), a linear mixed model was considered. The time metric used in the level 1 model was the baseline year 2006. The information about age at blood collection, sex, expanded CAG repeat length, age at onset and disease duration were used in the level 2 model to determine the relationship between blood transcript levels of *BCL2*, *BAX* and *TP53* as well as the *BCL2/BAX* ratio and the above-mentioned variables. The statistical analysis was performed using R software building on the longitudinal data analysis described by Garcia and colleagues [33]. Statistical significance was set at $p < 0.05$.

3. Results

3.1. Human Subjects

3.1.1. Reduced Transcript Levels of the Anti-Apoptotic *BCL2* Gene in Blood of MJD Patients

A cross-sectional study was conducted to evaluate if the transcript levels of *BCL2*, *BAX* and *TP53* are dysregulated in peripheral blood samples from total MJD subjects (Figure 2A) or in samples from subgroups of preclinical subjects, patients, and early patients, comparing with age- and sex-matched paired controls (Figure 2B,C). While comparison of patients with matched controls suggests reduced *BCL2* levels in MJD patients ($p = 0.041$) (Figure 2B), *BCL2* transcript abundance displays low accuracy to discriminate patients from matched controls (AUC = 0.64 (0.51–0.77), $p = 0.030$).

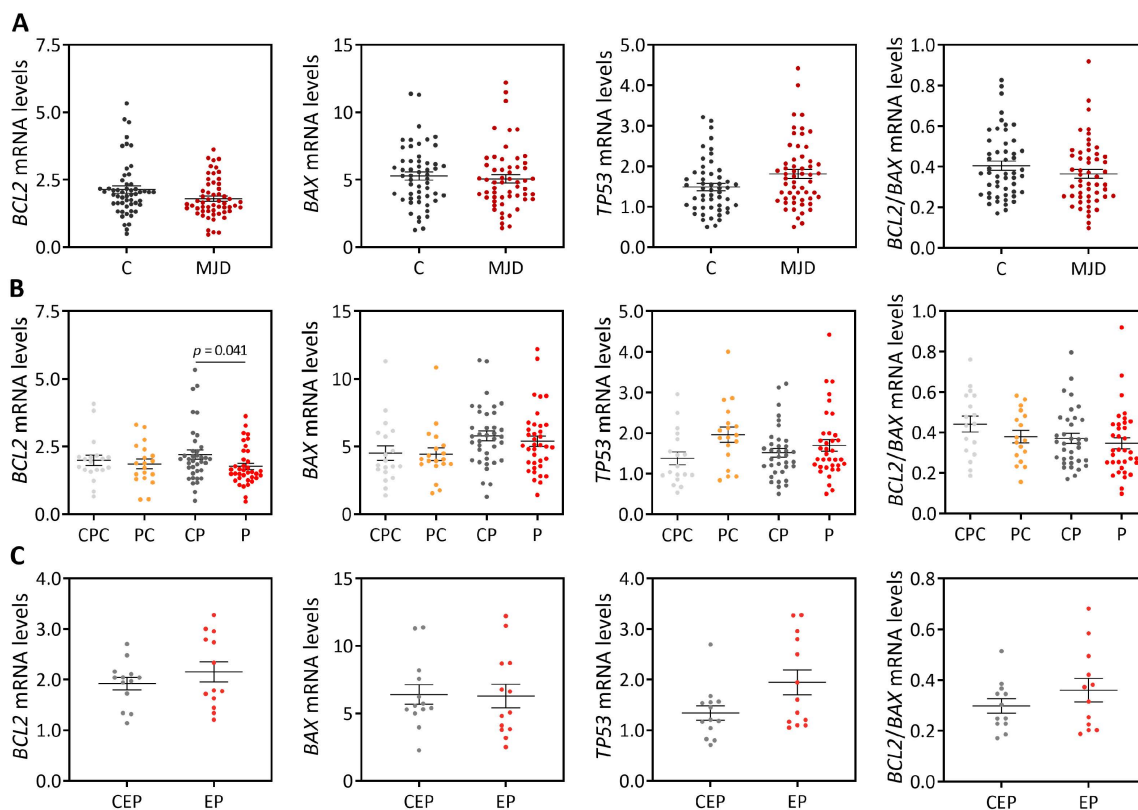


Figure 2. *BCL2*, *BAX* and *TP53* transcript levels and the *BCL2/BAX* ratio in peripheral blood samples from MJD carriers and controls: (A) Overall MJD subjects (dark red dots) were compared with matched controls (C, darkest grey dots). (B) Preclinical subjects (PC, orange dots) and patients (P, red dots) were compared to age- and sex-matched paired controls (CPC (dark grey dots) and CP (lightest grey dots), respectively). (C) Early patients (EP, light red dots) were compared with age- and sex-matched paired controls (CEP, light grey dots). Graphs show the mean and standard error mean of the $2^{-\Delta C_t}$ values. Dots represent mRNA levels for each individual.

3.1.2. Blood Samples of MJD Patients with Earlier Disease Onset Display Higher Levels of the Pro-Apoptotic *BAX* and Lower *BCL2/BAX* Ratio

Blood transcript levels of *BCL2*, *BAX* and *TP53* as well as the *BCL2/BAX* ratio were correlated with MJD subjects' demographic, genetic and clinical features (Supplementary Table S5). After adjusting for the age at blood collection and the number of CAG repeats in the expanded *ATXN3* allele, higher transcript levels of *BAX* and a lower *BCL2/BAX* ratio were observed in MJD patients with earlier onset ($\rho = -0.482$, $p = 0.003$ and $\rho = 0.393$, $p = 0.022$, respectively) (Supplementary Table S5).

3.1.3. Blood Anti-Apoptotic *BCL2* and Pro-Apoptotic *TP53* Transcript Levels Increase over Time in MJD Patients

Levels of *BCL2*, *BAX* and *TP53* blood transcripts were evaluated in samples from a subset of 18 MJD patients with at least two observation points during disease progression (Supplementary Figure S1). When adjusting a linear mixed model to the expression data of each of the three genes and to the *BCL2/BAX* ratio values, *TP53* levels increased on average 0.117 per year of disease (95% CI = 0.063–0.172, $p = 0.001$). Although in a lower extent, *BCL2* levels also increased on average 0.049 per year of disease (95% CI = 0.001–0.098, $p = 0.046$). Noteworthy, none of the possible confounding variables (age at blood collection, sex, expanded CAG repeat, age at disease onset and disease duration) influenced the observed increase in *TP53* and *BCL2* transcript abundance over time.

3.1.4. *BCL2/BAX* Ratio Is Increased in the Degenerative DCN and Pons of MJD Patients

The expression behavior of *BCL2*, *BAX*, *TP53* was next assessed at the transcript and protein levels in a small set of post-mortem brain samples from MJD patients and control individuals. Three brain regions of MJD patients were evaluated in this study: DCN and the pons which are greatly affected by degeneration in MJD patients [4], and the less affected frontal cortex [28,29]. Comparisons of transcript levels between MJD patients and controls for each brain region solely showed an increase in *BCL2/BAX* ratio in the DCN of patients ($p = 0.005$) (Figure 3).

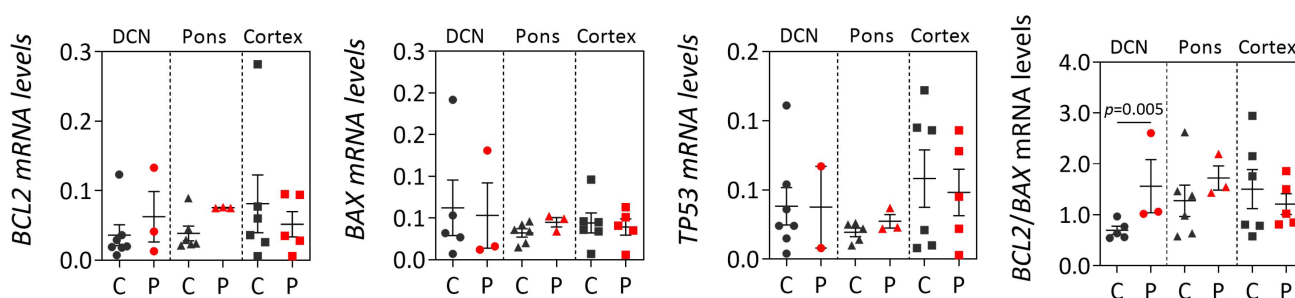


Figure 3. *BCL2*, *BAX* and *TP53* transcript levels and *BCL2/BAX* ratio in post-mortem brain regions (dentate cerebellar nucleus (DCN, circles), the pons (triangles) and frontal cortex (squares) from MJD patients (P, red dots) and controls (C, dark grey dots). Graphs show the mean and standard error of the mean of $2^{-\Delta Ct}$ values. Dots represent mRNA levels for each individual.

Next, protein levels of *BCL2*, *BAX* and *P53* were analyzed both in the soluble fraction (enriched in cytoplasmic proteins) and in the insoluble fraction (enriched in nuclear and insoluble proteins, including membrane proteins) of brain lysates (Figure 4; Supplementary Figure S2). In DCN, compared with controls, patients showed an increased *BCL2/BAX* ratio in the insoluble fraction ($p = 0.003$) (Figure 4A). In the pons, comparison between patients and controls revealed that patients show reduced soluble *BCL2* levels ($p = 0.004$) and subsequently decreased soluble *BCL2/BAX* ratio ($p = 0.028$), and higher insoluble *BCL2* levels ($p = 0.005$) and consequently increased of insoluble *BCL2/BAX* ratio ($p < 0.001$) (Figure 4B). In the frontal cortex, compared to controls, patients only showed increased soluble *BAX* levels ($p = 0.039$) (Figure 4C). Importantly, *BCL2/BAX* expression was increased in patients DCN both at the transcript and insoluble protein levels compared with healthy controls.

3.2. MJD Mouse Model

3.2.1. Abundance of *Bcl2*, *Bax* and *Trp53* Transcripts Is Similar in Blood and Brain Samples of Q84 and wt Mice

To determine whether Q84 mice replicate the blood transcriptional behavior of *BCL2*, *BAX* and *TP53* of preclinical subjects, the levels of their homologue genes were analyzed

in blood samples of pre-symptomatic 9 MO Q84 mice (without motor dysfunction [10]) and wt littermates. Like the observed in preclinical MJD subjects and matched controls, no significant differences of *Bcl2*, *Bax* and *Trp53* blood transcript levels or *Bcl2/Bax* ratio were found between pre-symptomatic 9 MO Q84 mice and wt mice (Figure 5A). Next, the levels of the three genes were evaluated in the pons and cerebral cortex (respectively, affected and mildly/non-affected regions by degeneration [30]) of pre-symptomatic 9 MO and symptomatic 18 MO Q84 mice [10] and wt littermate controls. As previously found in MJD patients' pons and frontal cortex samples, no differences of transcriptional levels were observed for the three evaluated genes in the two brain regions of Q84 mice (Figure 5B,C).

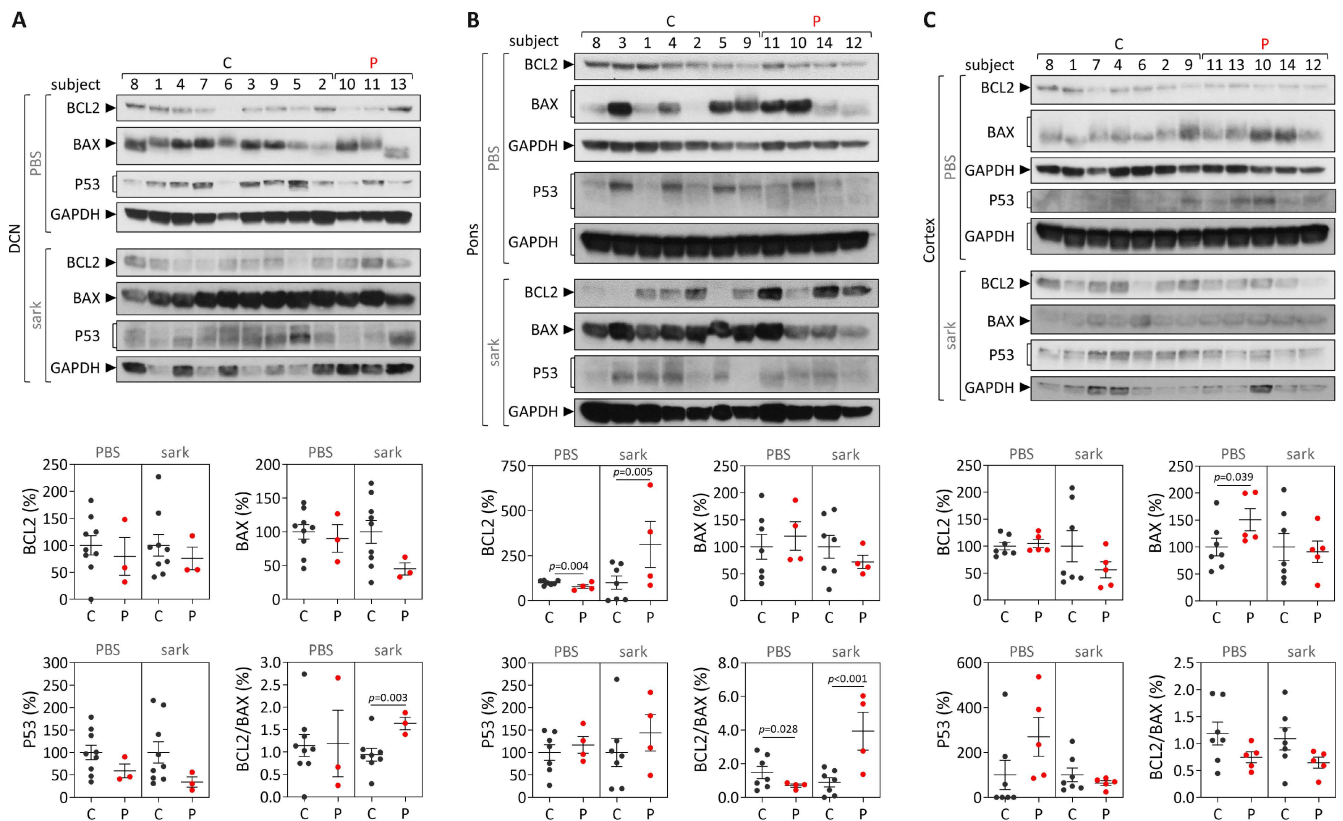


Figure 4. BCL2, BAX and P53 protein levels and BCL2/BAX ratio in post-mortem brains from MJD patients (P, red dots) and controls (C, dark grey dots). Protein levels in PBS-soluble (soluble) and sarkosyl-soluble (insoluble) fractions in (A) dentate cerebellar nucleus (DCN), (B) pons and (C) frontal cortex. Upper panels show immunoblots of indicated proteins in both soluble (PBS) and insoluble (sark) fractions. Lower panels display quantification of band intensity, with values normalized to GAPDH. Bars in the graphs represent the average percentage of protein relative to controls (\pm SEM). Dots represent protein levels for each individual.

3.2.2. The Pons and the Cerebral Cortex of Pre-Symptomatic Q84 Mice Show Evidence of Increased Abundance of Soluble Bax Protein but Similar Bcl2/Bax Ratios Comparing with Controls

Protein levels of Bcl2, Bax and p53 were analyzed in the soluble and insoluble fractions of brain lysates from the pons and cerebral cortex of pre-symptomatic 9 MO Q84 transgenic [10] and wt mice (Figure 6; Supplementary Figure S3). Compared with controls, while Q84 pons show evidence of increased soluble Bax levels ($p = 0.001$) and increased insoluble Bcl2 levels ($p = 0.003$) (Figure 6A), Q84 cerebral cortex only display increased soluble Bax levels ($p = 0.033$) (Figure 6B).

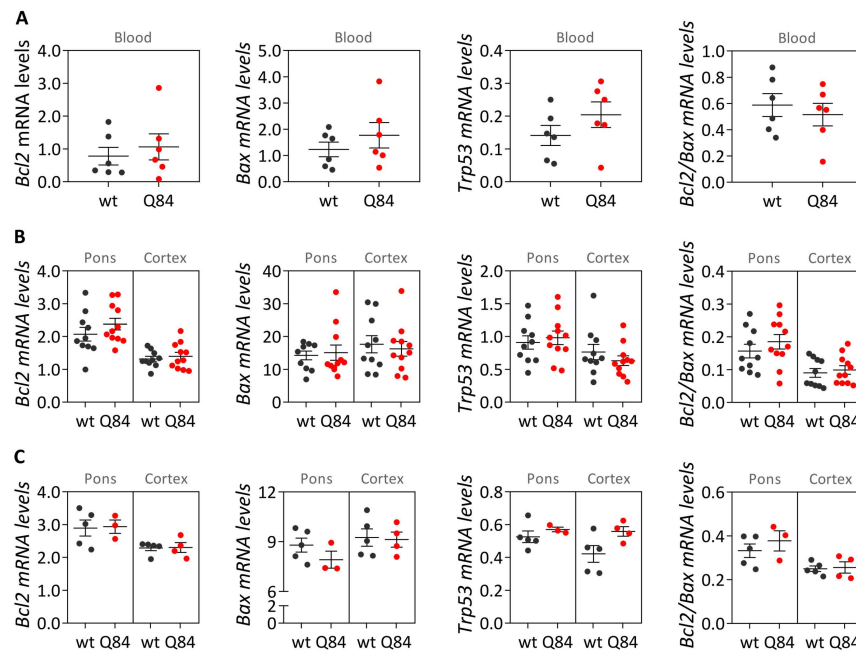


Figure 5. Transcript levels of *Bcl2*, *Bax* and *Trp53* and *Bcl2/Bax* ratio in pre-symptomatic 9 months-old (MO) (A,B) and symptomatic 18 MO (C) Q84 transgenic (red dots) and wt mice (dark grey dots). Transcript levels were analyzed in (A) blood samples and in (B) brain samples from pons and cerebral cortex of the same mice. Graphs show the mean and standard error of the mean of $2^{-\Delta Ct}$ values. Dots represent mRNA levels for each individual.

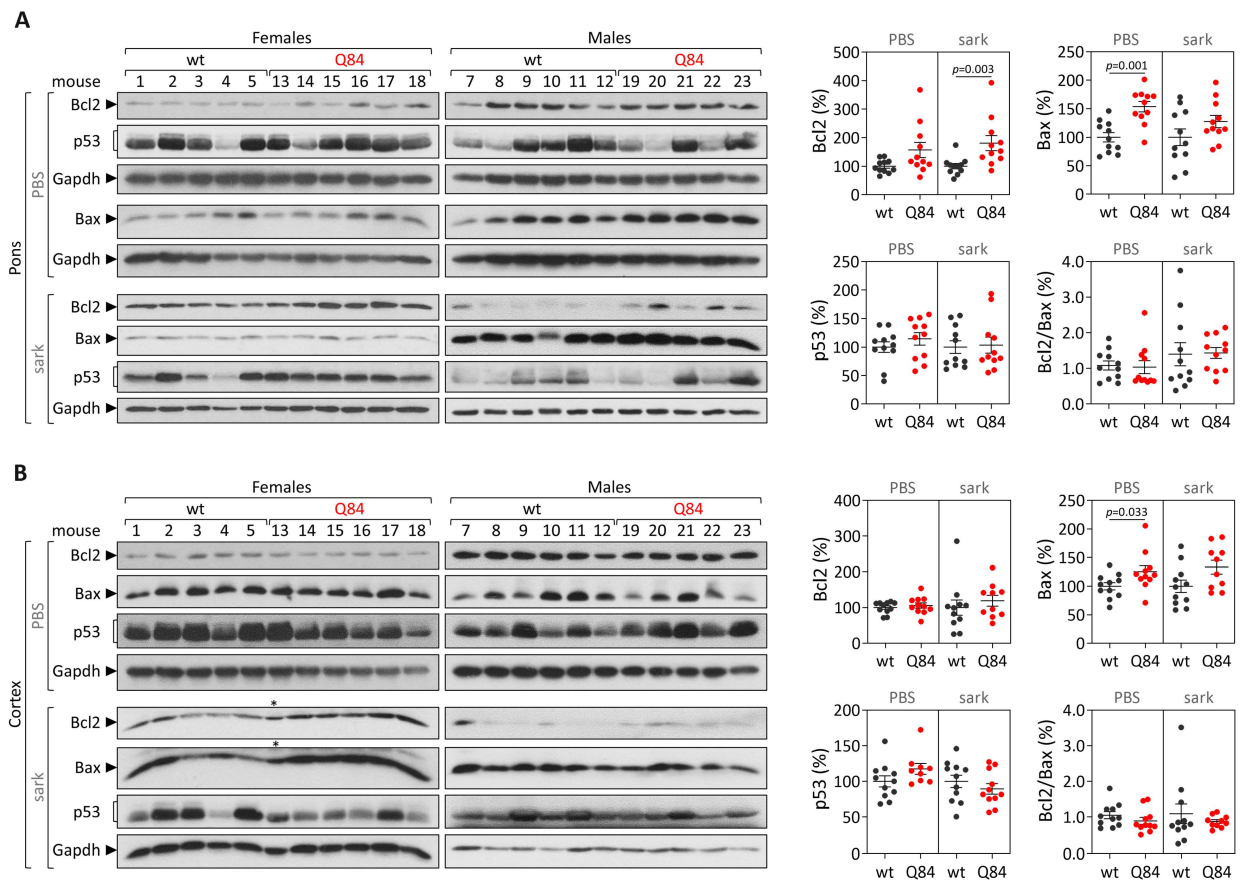


Figure 6. Protein levels of *Bcl2*, *Bax* and *p53* as well as *Bcl2/Bax* ratio in PBS-soluble (soluble) and sarkosyl-soluble (insoluble) fractions in (A) pons and (B) cerebral cortex of pre-symptomatic 9 MO

Q84 transgenic (red dots) and wt mice (dark grey dots). Left panels show immunoblots of indicated proteins in both soluble (PBS) and insoluble (sark) fractions. Right panels display the quantification of band intensity of all samples, with values normalized to GAPDH. Bars in the graphs represent the average percentage of protein relative to controls (\pm SEM). Dots represent protein levels for each individual. Samples labeled with a symbol (*) were excluded from statistical analysis.

3.2.3. Cerebral Cortex from Symptomatic Q84 Transgenic Mice Shows Evidence of Higher Insoluble Bcl2/Bax Ratio

Protein levels of Bcl2, Bax and p53 were further analyzed in the soluble and the insoluble fractions of the pons and cerebral cortex lysates from symptomatic 18 MO Q84 transgenic (showing motor impairment [10]) and controls. In the pons, comparison between symptomatic Q84 and wt mice shows evidence of reduced soluble Bax levels ($p = 0.014$) and a subsequent increase in soluble Bcl2/Bax ratio in Q84 transgenic mice ($p = 0.027$) (Figure 7A). In cerebral cortex, symptomatic Q84 mice solely display increased insoluble Bcl2/Bax ratio compared with wt mice ($p = 0.027$) (Figure 7B). These results contrast with the findings in the corresponding brain regions from the MJD patients (decreased soluble Bcl2/Bax ratio in the pons and increased insoluble Bcl2/Bax ratio in the frontal cortex).

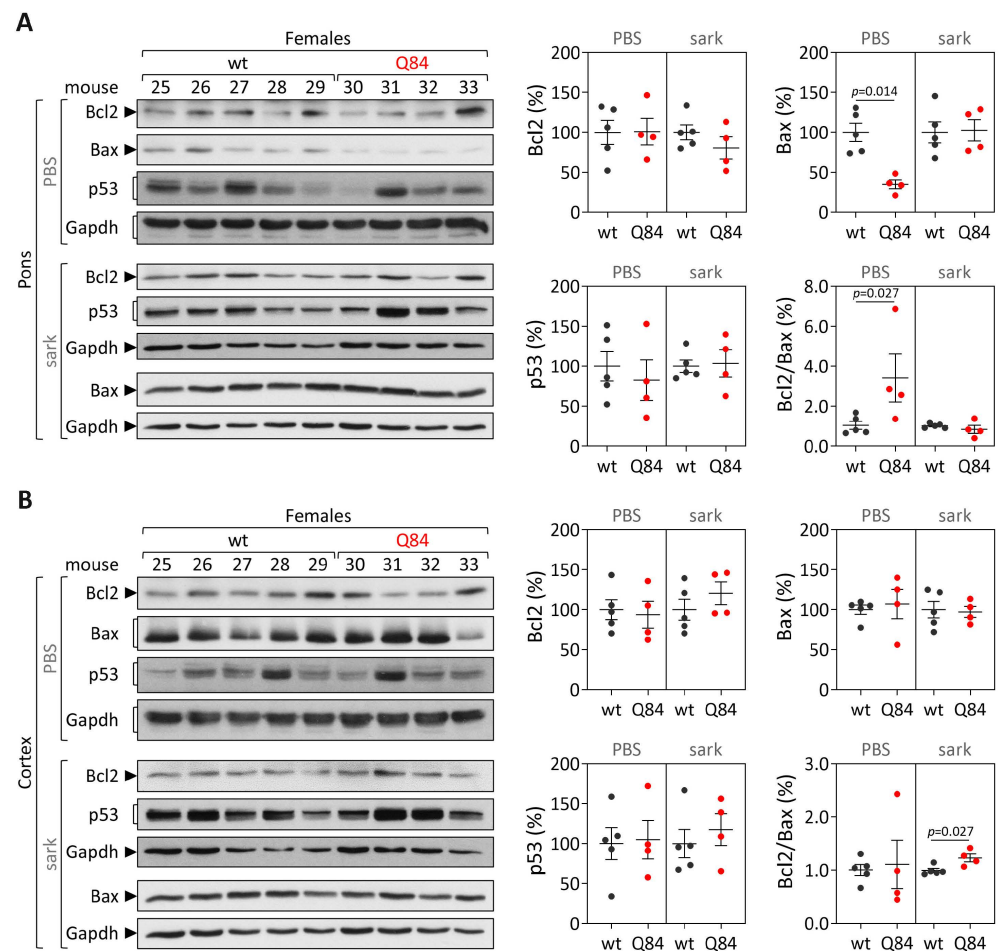


Figure 7. Protein levels of Bcl2, Bax and p53 as well as Bcl2/Bax ratio in PBS-soluble (soluble) and sarkosyl-soluble (insoluble) fractions in (A) pons and (B) cerebral cortex of symptomatic 18 MO Q84 transgenic (red dots) and wt mice (dark grey dots). Left panels show immunoblots of indicated proteins in both soluble (PBS) and insoluble (sark) fractions. Right panels display quantification of band intensity, with values normalized to GAPDH. Bars in the graphs represent the average percentage of protein relative to controls (\pm SEM). Dots represent protein levels for each individual.

4. Discussion

In this study, the expression behavior of the apoptosis-related genes *BCL2*, *BAX* and *TP53* and the *BCL2/BAX* ratio, an indicator of susceptibility to apoptosis [34], was evaluated in peripheral blood and post-mortem brain samples from MJD subjects and Q84 transgenic mice. Like previous reports [8,18], our cross-sectional analysis showed evidence of reduced *BCL2* transcript levels in blood of MJD patients. However, the abundance of blood *BCL2* transcripts revealed a low capacity to discriminate these two biological groups, thus precluding the use of *BCL2* levels as a biomarker of MJD. Similar blood *BCL2/BAX* transcript ratio was further found in MJD patients and matched controls, which contrasts with the previous report describing a reduced *BCL2/BAX* transcript ratio in MJD patients [8]. The partial replication of the published results [8] could perhaps be explained by the analysis of a small number of patients ($n = 37$) and the use of age- and sex-matched paired controls in this study comparing with the study by Raposo and colleagues analyzing a higher number of patients ($n = 74$) but non-matched controls [8]. In addition, similar blood abundance of *BCL2* transcripts and the *BCL2/BAX* transcript ratio was found here in MJD preclinical subjects and matched controls ($n = 19$), also contrasting with previous reports showing reduced *BCL2* levels [18] and the *BCL2/BAX* transcript ratio in the blood of preclinical subjects ($n = 16$) [8]. Again, the different observations in MJD preclinical subjects described here and in the previous reports [8,18] could be due to the use of different experimental designs, namely the use of age- and sex-matched paired controls in this study versus non-matched controls used in the published reports [8,18]. Noteworthy, in this study, increased levels of blood pro-apoptotic *BAX* transcripts and a decreased *BCL2/BAX* ratio were found to be associated with earlier age at onset, indicating that these transcriptional alterations may be associated with MJD pathogenesis. Consistently with these findings, and although global *TP53* levels are similar in patients and healthy controls, our follow-up analysis of blood samples from 18 MJD patients collected at distinct moments of disease progression over a maximum period of nine years showed that the abundance of pro-apoptotic *TP53* transcripts increases with disease progression. In contrast, and while in a lower extent than *TP53* transcript changes, levels of anti-apoptotic *BCL2* transcripts also increased with disease progression. The increased abundance of blood *TP53* and *BCL2* transcripts with MJD progression may indicate that pro-apoptotic and anti-apoptotic signs increase concomitantly in this tissue with the disease course.

While post-mortem brains from MJD patients are very rare, dispersed throughout several brain banks in the world and studies using such materials usually show a low power, the analysis of human MJD brain samples contributes to the elucidation of altered cellular mechanisms at the end stage of disease that may be associated with MJD pathogenesis. Overall, our cross-sectional findings of the increased *BCL2/BAX* transcript ratio in DCN and the increased insoluble protein *BCL2/BAX* ratio in DCN and the pons of post-mortem MJD brains suggest that, contrarily to what would be expected, cells in the DCN and pons, which are brain areas severely affected by degeneration in MJD [4,28,29] might be more prone to survive compared with controls. Interestingly, this behavior was not observed in the less-affected frontal cortex of MJD patients that only showed significantly increased soluble *BAX* levels, suggesting that this brain region displays similar susceptibility to apoptosis in MJD patients and in control individuals. The evidence of increased abundance of insoluble *BCL2/BAX* ratio observed in the DCN and pons of MJD patients may indicate increased abundance of the *BCL2* protein in the mitochondrial outer membrane thus preventing apoptosis activation by inhibiting the activity of pro-apoptotic *BCL2* family members [35]. However, the possibility that some of these insoluble proteins could instead be recruited to ATXN3 aggregates or be localized in other cellular membranes cannot be excluded. Yet, the results observed in the DCN and pons of MJD patients agree with previous reports of absence of TUNEL-positive cells and changes of expression of apoptosis-related proteins (*BCL2*, *P53*, *BAX* or *CPP32*) in post-mortem DCN from MJD patients [24]. MJD patients globally show a long survival time (time elapsed from onset to death) [36] and thus post-mortem MJD brain samples most likely represent end stages of the disease. Hence, the most

affected neurons and other cells in the DCN and pons of MJD patients [4] are most probably dead and absent at the end stage of disease and, therefore, the increased anti-apoptotic signs (BCL2/BAX ratio) observed in both brain regions could indicate that the surviving glial and neuronal cells in these two affected regions activate survival protection mechanisms at the end-stage of MJD. Similarly, Satou et al. [37] reported that the abundance of BCL2 protein within neurons of post-mortem brains from Alzheimer's disease patients increased with disease severity, suggesting that BCL2 protein may have a protective role at the end-stage of the disease.

In parallel with the study in human subjects, mouse *Bcl2*, *Bax* and *Trp53* transcript and protein levels were assessed in blood of pre-symptomatic 9 MO Q84 transgenic mice, and in the pons and cerebral cortex of both pre-symptomatic 9 MO and symptomatic 18 MO Q84 mice [10,30] to evaluate whether this widely used MJD mouse model replicates the findings observed in MJD subjects. Our cross-sectional analysis of Q84 mice, showed similar *Bcl2*, *Bax* and *Trp53* transcript levels in the blood of pre-symptomatic 9 MO Q84 mice and controls. These results in the pre-symptomatic Q84 mice agree with the observed lack of differences between the abundance of *BCL2*, *BAX* and *TP53* transcripts in peripheral blood samples from preclinical MJD subjects and age- and sex-matched paired controls. Additionally, similar transcript levels of *Bcl2*, *Bax* and *Trp53* were found in the pons and cerebral cortex of pre-symptomatic 9 MO or symptomatic 18 MO Q84 transgenic mice and wt controls. Interestingly, the similar abundance of the three assessed transcripts in the pons and cerebral cortex of symptomatic Q84 mice and controls mimics the observations in post-mortem brains from MJD patients further indicating that the Q84 mice replicate several aspects of the human disease. In contrast to the observed similar abundance of *Bcl2*, *Bax* and *Trp53* transcripts in pre-symptomatic and symptomatic Q84 and wt mice, altered levels of Bcl2 and/or Bax proteins were found in the two assessed brain regions of pre-symptomatic and symptomatic Q84 transgenic mice compared with wt littermates. Despite the altered abundance of these two proteins in the pons and cerebral cortex of pre-symptomatic 9 MO Q84 mice, the cells present in these brain regions show similar susceptibility to apoptosis as in controls, as shown by the similar insoluble Bcl2/Bax ratio. Likewise, cells in the pons of symptomatic 18 MO Q84 transgenic mice and controls show a similar susceptibility to apoptosis, while the cells in the less-affected cerebral cortex of symptomatic Q84 mice display increased levels of insoluble Bcl2/Bax ratio possibly indicating higher apoptosis resistance. In summary, pre-symptomatic and symptomatic Q84 transgenic mice show altered abundance of Bcl2 and Bax proteins with disease progression in both brain regions. Additionally, the similar results observed in the less-affected cerebral cortex of symptomatic 18 MO Q84 mice and in the severely affected the DCN and pons of MJD patients suggest that symptomatic Q84 mice are at different stages of the disease compared to post-mortem MJD brains. Globally, the mitochondrial apoptosis mechanisms in cells present in the highly affected and less-affected brain regions seem to respond differently in an age-dependent way to the damage elicited by the expanded *ATXN3* CAG repeat in MJD.

Overall, our study displays some limitations such as the limited statistical power of the analysis of post-mortem brain samples due to the small sample size, and the lack of blood transcript levels over disease progression in Q84 transgenic mice due to the lack of peripheral blood samples from symptomatic 18 MO transgenic Q84 mice. The fact that no transcriptional differences were found in the Q84 mouse model suggests that this animal model may replicate the human disease, yet future studies using mouse samples from several points along disease progression would need to be performed to test this hypothesis. Importantly, future evaluation of the abundance of a wider number of apoptotic-related molecules including markers of the late phase of apoptosis in peripheral blood samples from MJD subjects and post-mortem MJD brains could reveal novel biomarkers of MJD and could help elucidate the apoptotic signaling cascades that are majorly involved in MJD. Lastly, because mutant *ATXN3* stabilizes P53 leading to an increased abundance of p53 in MJD cellular models [21], future quantification of the P53 protein in peripheral blood from MJD carriers could reveal a new progression biomarker for MJD.

5. Conclusions

Globally, our findings indicate that there is tissue-specific vulnerability to apoptosis in MJD subjects and that this tissue-dependent behavior is only partially replicated by the MJD Q84 mouse model.

Supplementary Materials: The following supporting information can be downloaded at <https://www.mdpi.com/article/10.3390/cells12101404/s1>: Table S1: Characterization of the MJD subjects (preclinical subjects and patients) and control individuals used in this study (n = 124), Table S2: Demographic, genetic, and clinical data of the 18 MJD patients used in the follow-up study, Table S3: Characterization of post-mortem human brain samples from MJD patients and controls individuals, and RNA integrity number of each brain samples used in this study, Table S4: Genotypes of the 9 and 18 month-old mice used in this study, Table S5: Correlations between transcript levels of *BCL2*, *BAX* and *TP53*, and *BCL2/BAX* ratio, and demographic, genetic and clinical data of MJD subjects (preclinical individuals and patients), Figure S1: *BCL2*, *BAX* and *TP53* transcriptional levels and *BCL2/BAX* ratio changes over time in the 18 MJD patients analyzed in the follow-up study, Figure S2: Western blot using the anti-ATXN3 antibody (1H9) to detect the native human ATXN3 (nATXN3) and expanded human ATXN3 (eATXN3) in insoluble protein fraction of post-mortem human samples from dentate cerebellar nucleus (DCN), pons and frontal cortex (Cortex) of Machado-Joseph disease patients (P) and control subjects (C). GAPDH was used as a protein loading control, Figure S3: Western blot using the anti-ATXN3 antibody (1H9) to detect the mutant human ATXN3 (hATXN3) and endogenous mouse ATXN3 (eATXN3) in soluble fraction of protein from (A) cerebral cortex of 9 months-old and (B) 18 months-old hemizygous YACMJD84.2 (Q84) transgenic and wild-type (wt) littermate mice. GAPDH was used as a protein loading control.

Author Contributions: Conceptualization, M.R., M.d.C.C. and M.L.; Methodology, A.F.F., M.R., M.d.C.C. and M.L.; Validation, A.F.F., M.d.C.C. and M.L.; Formal Analysis, A.F.F., M.d.F.B., M.d.C.C. and M.L.; Investigation, A.F.F., M.R., E.D.S., N.S.A., F.M., M.d.F.B., M.P., J.V., T.K., M.d.C.C. and M.L.; Resources, M.d.C.C. and M.L.; Writing—Original Draft Preparation, A.F.F., M.d.C.C. and M.L.; Writing—Review and Editing, A.F.F., M.R., E.D.S., N.S.A., F.M., M.d.F.B., M.P., J.V., T.K., M.d.C.C. and M.L.; Visualization, A.F.F., M.d.C.C. and M.L.; Supervision, M.d.C.C. and M.L.; Project Administration, M.d.C.C. and M.L.; Funding Acquisition, M.d.C.C. and M.L. All authors have read and agreed to the published version of the manuscript.

Funding: This work was funded by FEDER funds through the Operational Competitiveness Program (COMPETE) and by National Funds through Fundação para a Ciência e a Tecnologia (FCT) under the project FCOMP-01-0124-FEDER-028753 (PTDC/DTP/PIC/0370/2012) and was also funded by National Ataxia Foundation through a research seed money grant (2018). A.F.F. was supported by PhD grant (SFRH/BD/121101/2016) funded by FCT, República Portuguesa/Ciência, Tecnologia e Ensino Superior, Portugal 2020, União Europeia/Fundo Social Europeu and POR_NORTE. MR is supported by FCT (CEECIND/03018/2018). M.d.C.C. was supported by the Heeringa Ataxia Research fund (University of Michigan). M.d.F.B. research was partially supported by National Funds through FCT—Fundação para a Ciência e Tecnologia, project UIDB/00006/2020 (CEAUL).

Institutional Review Board Statement: The study was conducted according to the guidelines of the Declaration of Helsinki. Blood samples from MJD subjects and controls were collected in the scope of the projects MESCA3 (PTDC/DTP-PIC/0370/2012), approved by the Ethical Committee of the Hospital do Divino Espírito Santo. The use of post-mortem human brain samples was approved by the University of Michigan Biosafety Committee (IBCA00000265, 7 March 2017). Animal procedures were approved by the University of Michigan Committee on Use and Care of Animals (Protocol PRO00006371, 6 October 2015). Project research seed money grant “Apoptosis-related genes *BCL2*, *BAX* and *TP53* as biomarkers of Machado-Joseph Disease”, approved by the Ethical Committee of the University of the Azores (PARECER 26/2018, 25 September 2018) and by the University of Michigan (AWD006601, 9 January 2018).

Informed Consent Statement: Informed consent was obtained from all subjects involved in the study.

Data Availability Statement: The data presented in this study are available on request from the corresponding author.

Acknowledgments: We are grateful to the MJD subjects and their relatives as well as to the healthy volunteers for participating in this study. We thank Ilya Bezprozvanny for sharing the YACMJD84.2 mice. The Michigan brain bank at the University of Michigan is partially supported by the NIH/NIA funded Michigan Alzheimer’s Disease Center (P30AG053760 and P30AG072931).

Conflicts of Interest: The authors declare no conflict of interest.

References

1. Klockgether, T.; Mariotti, C.; Paulson, H.L. Spinocerebellar Ataxia. *Nat. Rev. Dis. Prim.* **2019**, *5*, 24. [[CrossRef](#)]
2. Kawaguchi, Y.; Okamoto, T.; Taniwaki, M.; Aizawa, M.; Inoue, M.; Katayama, S.; Kawakami, H.; Nakamura, S.; Nishimura, M.; Akiguchi, I. CAG Expansions in a Novel Gene for Machado-Joseph Disease at Chromosome 14q32.1. *Nat. Genet.* **1994**, *8*, 221–228. [[CrossRef](#)] [[PubMed](#)]
3. Costa, M.d.C.; Paulson, H.L. Toward Understanding Machado–Joseph Disease. *Prog. Neurobiol.* **2012**, *97*, 239–257. [[CrossRef](#)]
4. Rüb, U.; Brunt, E.R.; Deller, T. New Insights into the Pathoanatomy of Spinocerebellar Ataxia Type 3 (Machado-Joseph Disease). *Curr. Opin. Neurol.* **2008**, *21*, 111–116. [[CrossRef](#)]
5. Bettencourt, C.; Lima, M. Machado-Joseph Disease: From First Descriptions to New Perspectives. *Orphanet J. Rare Dis.* **2011**, *6*, 35. [[CrossRef](#)]
6. Wu, X.; Liao, X.; Zhan, Y.; Cheng, C.; Shen, W.; Huang, M.; Zhou, Z.; Wang, Z.; Qiu, Z.; Xing, W.; et al. Microstructural Alterations in Asymptomatic and Symptomatic Patients with Spinocerebellar Ataxia Type 3: A Tract-Based Spatial Statistics Study. *Front. Neurol.* **2017**, *8*, 714. [[CrossRef](#)]
7. Rezende, T.J.R.; de Paiva, J.L.R.; Martinez, A.R.M.; Lopes-Cendes, I.; Pedroso, J.L.; Barsottini, O.G.P.; Cendes, F.; Franca, M.C.J. Structural Signature of SCA3: From Presymptomatic to Late Disease Stages. *Ann. Neurol.* **2018**, *84*, 401–408. [[CrossRef](#)] [[PubMed](#)]
8. Raposo, M.; Ramos, A.; Santos, C.; Kazachkova, N.; Teixeira, B.; Bettencourt, C.; Lima, M. Accumulation of Mitochondrial DNA Common Deletion Since The Preataxic Stage of Machado-Joseph Disease. *Mol. Neurobiol.* **2019**, *56*, 119–124. [[CrossRef](#)] [[PubMed](#)]
9. Wilke, C.; Haas, E.; Reetz, K.; Faber, J.; Garcia-Moreno, H. Neurofilaments as Blood Biomarkers at the Preataxic and Ataxic Stage of Spinocerebellar Ataxia Type 3: A Cross-Species Analysis in Humans and Mice. *EMBO Mol. Med.* **2020**, *12*, e11803. [[CrossRef](#)]
10. Do Carmo Costa, M.; Luna-Cancelon, K.; Fischer, S.; Ashraf, N.S.; Ouyang, M.; Dharia, R.M.; Martin-Fishman, L.; Yang, Y.; Shakkottai, V.G.; Davidson, B.L.; et al. Toward RNAi Therapy for the Polyglutamine Disease Machado-Joseph Disease. *Mol. Ther.* **2013**, *21*, 1898–1908. [[CrossRef](#)]
11. Rodriguez-Lebron, E.; Costa, M.d.C.; Luna-Cancelon, K.; Peron, T.M.; Fischer, S.; Boudreau, R.L.; Davidson, B.L.; Paulson, H.L. Silencing Mutant ATXN3 Expression Resolves Molecular Phenotypes in SCA3 Transgenic Mice. *Mol. Ther.* **2013**, *21*, 1909–1918. [[CrossRef](#)] [[PubMed](#)]
12. Moore, L.R.; Rajpal, G.; Dillingham, I.T.; Qutob, M.; Blumenstein, K.G.; Gattis, D.; Hung, G.; Kordasiewicz, H.B.; Paulson, H.L.; McLoughlin, H.S. Evaluation of Antisense Oligonucleotides Targeting ATXN3 in SCA3 Mouse Models. *Mol. Ther. Nucleic Acids* **2017**, *7*, 200–210. [[CrossRef](#)] [[PubMed](#)]
13. McLoughlin, H.S.; Moore, L.R.; Chopra, R.; Komlo, R.; McKenzie, M.; Blumenstein, K.G.; Zhao, H.; Kordasiewicz, H.B.; Shakkottai, V.G.; Paulson, H.L. Oligonucleotide Therapy Mitigates Disease in Spinocerebellar Ataxia Type 3 Mice. *Ann. Neurol.* **2018**, *84*, 64–77. [[CrossRef](#)] [[PubMed](#)]
14. Ashraf, N.S.; Duarte-Silva, S.; Shaw, E.D.; Maciel, P.; Paulson, H.L.; Teixeira-Castro, A.; Costa, M.d.C. Citalopram Reduces Aggregation of ATXN3 in a YAC Transgenic Mouse Model of Machado-Joseph Disease. *Mol. Neurobiol.* **2019**, *56*, 3690–3701. [[CrossRef](#)]
15. Evers, M.M.; Toonen, L.J.A.; Van Roon-Mom, W.M.C. Ataxin-3 Protein and RNA Toxicity in Spinocerebellar Ataxia Type 3: Current Insights and Emerging Therapeutic Strategies. *Mol. Neurobiol.* **2014**, *49*, 1513–1531. [[CrossRef](#)]
16. Schuster, K.H.; Zalon, A.J.; Zhang, H.; DiFranco, D.M.; Stec, N.R.; Haque, Z.; Blumenstein, K.G.; Pierce, A.M.; Guan, Y.; Paulson, H.L.; et al. Impaired Oligodendrocyte Maturation Is an Early Feature in SCA3 Disease Pathogenesis. *J. Neurosci.* **2022**, *42*, 1604–1617. [[CrossRef](#)]
17. Raposo, M.; Bettencourt, C.; Maciel, P.; Gao, F.; Ramos, A.; Kazachkova, N.; Vasconcelos, J.; Kay, T.; Rodrigues, A.J.; Bettencourt, B.; et al. Novel Candidate Blood-Based Transcriptional Biomarkers of Machado-Joseph Disease. *Mov. Disord.* **2015**, *30*, 968–975. [[CrossRef](#)]
18. Raposo, M. Predicting and Tracking Machado-Joseph Disease: Biomarkers of Diagnosis and Prognosis. Ph.D. Thesis, Universidade dos Açores, Ponta Delgada, Portugal, 2016.
19. Chipuk, J.E.; Moldoveanu, T.; Llambi, F.; Parsons, M.J.; Green, D.R. The BCL-2 Family Reunion. *Mol. Cell* **2010**, *37*, 299–310. [[CrossRef](#)]
20. Fridman, J.S.; Lowe, S.W. Control of Apoptosis by P53. *Oncogene* **2003**, *22*, 9030–9040. [[CrossRef](#)]
21. Liu, H.; Li, X.; Ning, G.; Zhu, S.; Ma, X.; Liu, X.; Liu, C.; Huang, M.; Schmitt, I.; Wüllner, U.; et al. The Machado–Joseph Disease Deubiquitinase Ataxin-3 Regulates the Stability and Apoptotic Function of P53. *PLoS Biol.* **2016**, *14*, e2000733. [[CrossRef](#)]
22. Tsai, H.F.; Tsai, H.J.; Hsieh, M. Full-Length Expanded Ataxin-3 Enhances Mitochondrial-Mediated Cell Death and Decreases Bcl-2 Expression in Human Neuroblastoma Cells. *Biochem. Biophys. Res. Commun.* **2004**, *324*, 1274–1282. [[CrossRef](#)] [[PubMed](#)]

23. Chou, A.H.; Yeh, T.H.; Kuo, Y.L.; Kao, Y.C.; Jou, M.J.; Hsu, C.Y.; Tsai, S.R.; Kakizuka, A.; Wang, H.L. Polyglutamine-Expanded Ataxin-3 Activates Mitochondrial Apoptotic Pathway by Upregulating Bax and Downregulating Bcl-XL. *Neurobiol. Dis.* **2006**, *21*, 333–345. [[CrossRef](#)]
24. Kumada, S.; Hayashi, M.; Mizuguchi, M.; Nakano, I.; Morimatsu, Y.; Oda, M. Cerebellar Degeneration in Hereditary Dentatorubral-Pallidoluysian Atrophy and Machado-Joseph Disease. *Acta Neuropathol.* **2000**, *99*, 48–54. [[CrossRef](#)] [[PubMed](#)]
25. Klockgether, T.; Lüdtke, R.; Kramer, B.; Abele, M.; Bürk, K.; Schöls, L.; Riess, O.; Laccone, F.; Boesch, S.; Lopes-Cendes, I.; et al. The Natural History of Degenerative Ataxia: A Retrospective Study in 466 Patients. *Brain* **1998**, *121*, 589–600. [[CrossRef](#)] [[PubMed](#)]
26. Raposo, M.; Ramos, A.; Bettencourt, C.; Lima, M. Replicating Studies of Genetic Modifiers in Spinocerebellar Ataxia Type 3: Can Homogeneous Cohorts Aid? *Brain* **2015**, *138*, e398. [[CrossRef](#)]
27. Bettencourt, C.; Fialho, R.N.; Santos, C.; Montiel, R.; Bruges-Armas, J.; Maciel, P.; Lima, M. Segregation Distortion of Wild-Type Alleles at the Machado-Joseph Disease Locus: A Study in Normal Families from the Azores Islands (Portugal). *J. Hum. Genet.* **2008**, *53*, 333–339. [[CrossRef](#)]
28. de Rezende, T.J.R.; D’Abreu, A.; Guimaraes, R.P.; Lopes, T.M.; Lopes-Cendes, I.; Cendes, F.; Castellano, G.; Franca, M.C.J. Cerebral Cortex Involvement in Machado-Joseph Disease. *Eur. J. Neurol.* **2015**, *22*, 277–e24. [[CrossRef](#)]
29. Arruda, W.O.; Meira, A.T.; Ono, S.E.; de Carvalho Neto, A.; Betting, L.E.G.G.; Raskin, S.; Camargo, C.H.F.; Teive, H.A.G. Volumetric MRI Changes in Spinocerebellar Ataxia (SCA3 and SCA10) Patients. *Cerebellum* **2020**, *19*, 536–543. [[CrossRef](#)]
30. Cemal, C.K. YAC Transgenic Mice Carrying Pathological Alleles of the MJD1 Locus Exhibit a Mild and Slowly Progressive Cerebellar Deficit. *Hum. Mol. Genet.* **2002**, *11*, 1075–1094. [[CrossRef](#)]
31. Ferreira, A.F.; Raposo, M.; Vasconcelos, J.; Costa, M.d.C.; Lima, M. Selection of Reference Genes for Normalization of Gene Expression Data in Blood of Machado-Joseph Disease/Spinocerebellar Ataxia Type 3 (MJD/SCA3) Subjects. *J. Mol. Neurosci.* **2019**, *3*, 450–455. [[CrossRef](#)]
32. Livak, K.J.; Schmittgen, T.D. Analysis of Relative Gene Expression Data Using Real-Time Quantitative PCR and the $2^{-\Delta\Delta C_T}$ Method. *Methods* **2001**, *25*, 402–408. [[CrossRef](#)] [[PubMed](#)]
33. Garcia, T.P.; Marder, K. Statistical Approaches to Longitudinal Data Analysis in Neurodegenerative Diseases: Huntington’s Disease as a Model. *Curr. Neurol. Neurosci. Rep.* **2017**, *17*, 14. [[CrossRef](#)]
34. Siddiqui, W.A.; Ahad, A.; Ahsan, H. The Mystery of BCL2 Family: Bcl-2 Proteins and Apoptosis: An Update. *Arch. Toxicol.* **2015**, *89*, 289–317. [[CrossRef](#)] [[PubMed](#)]
35. Lindsay, J.; Esposti, M.D.; Gilmore, A.P. Bcl-2 Proteins and Mitochondria—Specificity in Membrane Targeting for Death. *Biochim. Biophys. Acta—Mol. Cell Res.* **2011**, *1813*, 532–539. [[CrossRef](#)] [[PubMed](#)]
36. Kieling, C.; Prestes, P.R.; Saraiva-Pereira, M.L.; Jardim, L.B. Survival Estimates for Patients with Machado-Joseph Disease (SCA3). *Clin. Genet.* **2007**, *72*, 543–545. [[CrossRef](#)]
37. Satou, T.; Cummings, B.J.; Cotman, C.W. Immunoreactivity for Bcl-2 Protein within Neurons in the Alzheimer’s Disease Brain Increases with Disease Severity. *Brain Res.* **1995**, *697*, 35–43. [[CrossRef](#)]

Disclaimer/Publisher’s Note: The statements, opinions and data contained in all publications are solely those of the individual author(s) and contributor(s) and not of MDPI and/or the editor(s). MDPI and/or the editor(s) disclaim responsibility for any injury to people or property resulting from any ideas, methods, instructions or products referred to in the content.